World Conference on Timber Engineering Oslo 2023

EXPERIMENTAL STUDY ON LATERAL PERFORMANCE OF A FRAME WITH DEEP BEAMS AND HANGING MUD WALLS IN TRADITIONAL JAPANESE RESIDENTIAL HOUSES

Zherui Li[1], Hiroshi Isoda[2], Akihisa Kitamori[3], Takafumi Nakagawa[4], Yasuhiro Araki[5]

ABSTRACT: This study aimed to investigate the resistance of a frame with deep beams and hanging mud walls, clarify the working mechanisms and contributions of different load-bearing elements in the frame. A series of comparative experiments of the frames with and without hanging mud walls were carried out in the first step, as well as frames with hanging mud walls of different height aspect ratios. The contributions of main load-bearing elements, including mortise-tenon joints, deep beams, and hanging mud walls, were identified. Secondly, the performance of the deep beam and beam-column joints were discussed. Additionally, the parameter analysis of the height aspect ratios of hanging mud walls was also performed combined with component tests.

KEYWORDS: Traditional timber structure, Lateral resistance, Hanging mud wall, deep beam, interior notch

1 INTRODUCTION

Timber frame composites with mud walls constitute the basic structure for resisting lateral forces and are widely employed in both traditional oriental temples and castles in Japan. Specifically, the composition of hanging mud walls and deep beams have been promoted for use in traditional Japanese residential houses since 17th century (Edo-era) [1]. Due to the requirement of space permeability, the proportion of large-scale shear walls is relatively reduced and partially replaced by large-section timber frames with hanging walls in traditional-style houses (Figure 1). However, this practice may cause the risk of insufficient shear capacity according to current seismic design standards.

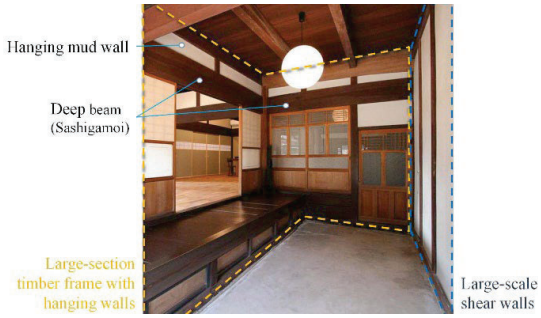

Figure 1: *Common structural systems in traditional Japanese residential houses.*

From the perspective of reinforcement of existing buildings, an accurate evaluation of the seismic performance of original structures is required for the need to maintain the appearance and minimize the expense in traditional residential houses. While the overall resistance of a frame with hanging wall height less than 750mm is underestimated according to the current seismic assessment method [2, 3], the resistance of mortise-tenon joints and deep beams are also not clearly involved in the evaluation of traditional residences in Japan. Simultaneously, considering that the shear force generated by hanging mud walls and deep beams and the moment of mortise-tenon joints all act on the column body and easily lead to bending deformation, the bending capacity of columns should be reassessed as a limiting factor of the drift-resisting capacity of the frame.

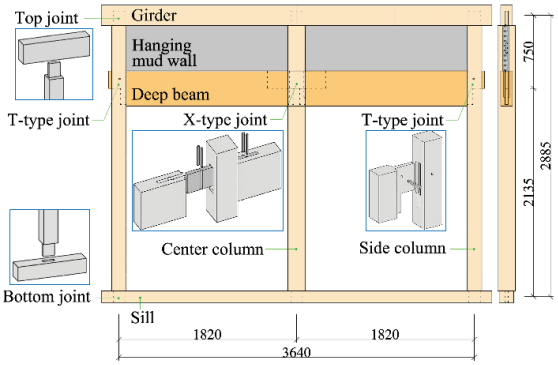

Figure 2: *Object frame with deep beams and hanging mud walls.*

[1] Zherui Li, College of Civil Engineering, Xi'an University of Architecture and Technology, China, lzr_6527@163.com
[2] Hiroshi Isoda, Research Institute for Sustainable Humanosphere, Kyoto University, Japan
[3] Akihisa Kitamori, Faculty of Engineering, Osaka Sangyo University, Japan
[4] Takafumi Nakagawa, Research Institute for Sustainable Humanosphere, Kyoto University, Japan
[5] Yasuhiro Araki, National Institute for Land and Infrastructure Management, Japan

https://doi.org/10.52202/069179-0527

This study took the double-span frame with deep beams and hanging mud walls as the object (Figure 2) and investigated the working mechanisms and contributions of different load-bearing elements, including mortise-tenon joints, deep beams, and hanging mud walls. Then the influence of different wall heights on lateral resistance capacity and damage mode of the frame were discussed based on comparative experiments.

2 EXPERIMENT

2.1 FRAME TESTS

With the purpose of visualizing the load-bearing mechanism and the contribution of the structural elements, in-plane static cyclic tests were conducted on frames with and without hanging mud walls, marked as *FW-M* and *F-M*, respectively. Then, to grasp the resistance of hanging mud walls with different heights, comparative experiments were conducted on frames with hanging mud walls of two height aspect ratios, marked as *FW-S* and *FW-L*, respectively. The dimension of frame specimens and mortise- tenon joints are shown in Figures 3 and 4.

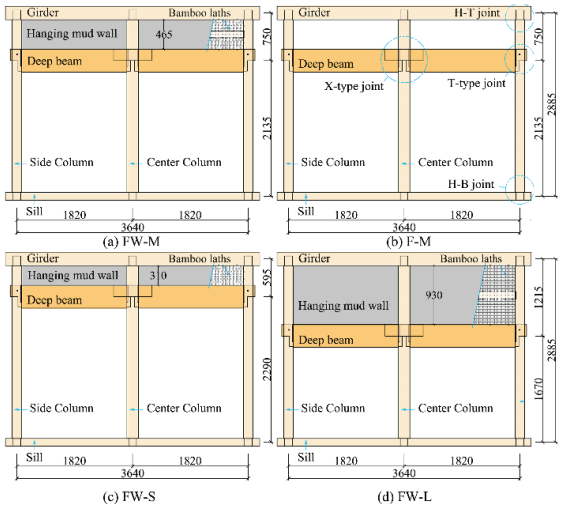

Figure 3: *Frame specimens (Unit: mm).*

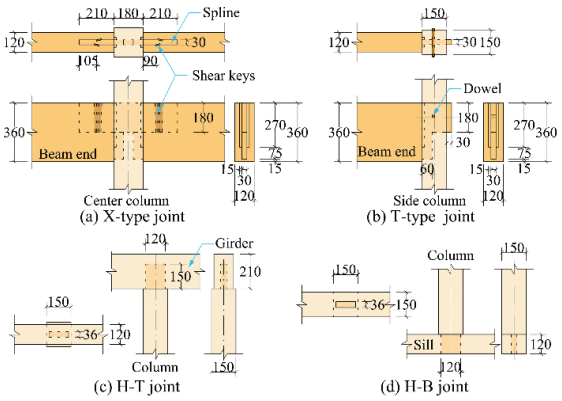

Figure 4: *Mortise-tenon joints in frame specimens (Unit: mm).*

For specimen FW-S, the clear height of the hanging mud wall was 310 mm. For specimens FW-M and FW-L, the wall height increased to 465 mm (1.5 times) and 930 mm (3 times). The aggregate thickness of the hanging mud wall was 70 mm, including the 40 mm thickness of rough-coated mud and 15 mm thickness of intermediate-coated mud. The dimensions, wood species and material properties of timber components in frame specimens are listed in Tables 1and 2.

Loading procedures of two groups of frame specimens were adapted from the standard ISO 16670. Cyclic load was applied along the centreline of the girder. Frame specimens were loaded with nine phases, each containing three fully revised cycles of equal amplitude. Target shear angles are raised from ±1/450, 1/300, 1/200, 1/150, 1/100, 1/75, 1/50, 1/30, to 1/15 rad, and then the load was added until the displacement limit of the hydraulic jack (approximately 1/10 rad) along the pull direction. Tie rods were installed along the side columns to control the vertical displacement and rotation of the frame, and the sill beam was fixed by sliding limit blocks.

Table 4: *Dimensions and wood species of members in frame specimens.*

Member	Dimension (mm)	Wood species
Side column	150×150×2720	Japanese cedar
Center Column	180×180×2720	Japanese cedar
Deep beam	120×360×1655	Douglas fir
Girder	150×210×4000	Japanese cedar
Sill	150×120×4000	Japanese cypress
Dowel	15×15×170	Oak
Shear key	6.5×30×135	Oak

Table 5: *Material properties of members in frame specimens.*

Category	Members	F-M	FW-M	FW-S	FW-L
MOE (kN/mm^2)	Column	8.72	8.75	8.69	8.84
	Deep beam	15.82	14.64	11.17	11.08
	Girder	9.69	8.01	10.30	8.83
	Sill	13.65	13.00	13.64	14.63
ρ (g/cm^3)	Column	0.41	0.40	0.39	0.40
	Deep beam	0.57	0.57	0.51	0.51
	Girder	0.41	0.43	0.41	0.40
	Sill	0.53	0.54	0.58	0.48
MC (%)	Column	19.6	20.0	19.2	20.6
	Deep beam	14.3	13.8	13.5	11.2
	Girder	19.6	20.3	18.2	17.4
	Sill	20.0	22.6	22.4	23.0

2.2 ELEMENTAL TESTS

To clarify the resistance contribution and deformation characteristics of the main components in the frame, including the rotational performance of mortise-tenon joints, shear resistance of deep beams and hanging mud walls, as well as the bending performance of columns with mortise, elemental tests were carried out and compared with frame tests.

https://doi.org/10.52202/069179-0527

Cyclic loading tests on two types of mortise-tenon joints of column and deep beam connections, the column top and bottom joints, the single-span frame containing a deep beam and two side columns, and mud wall elements with different heights corresponding to frame tests (310 mm, 465 mm, 930 mm) were conducted (Figure 5). Loading protocol of all these elemental tests were all consistent with the frame tests. Then 3-point bending tests of columns with mortise were performed.

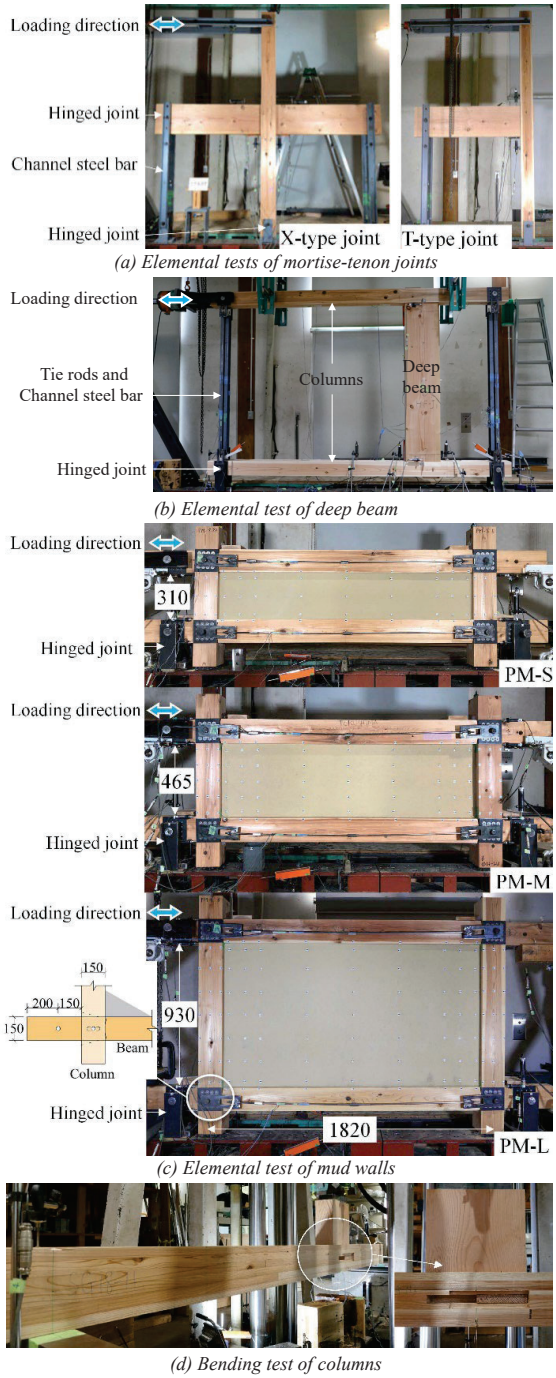

(a) Elemental tests of mortise-tenon joints

(b) Elemental test of deep beam

(c) Elemental test of mud walls

(d) Bending test of columns

Figure 5: *Elemental tests of main components in the frame.*

3 RESULTS AND DISCUSSION

3.1 LATERAL FORCE RESISTANCE OF OBJECT FRAMES

3.1.1 Observed damage

When the bare timber frame specimen F-M deformed under lateral force, there was an evident relative rotation between the columns and horizontal members (girder, deep beams, and sill). The effective length of deep beams gradually changed into the diagonal length and squeezed the columns on both sides. Although no obvious damage of joints or main components was observed even under a large displacement angle (1/10 rad), the outwardly bending tendency of both left- and right-side columns was very clearly observed. For specimen FW-M in contrast, the bending deformation of columns was not as significant as specimen F-M because of the restraint effect of hanging mud walls. Correspondingly, crushes of the left and right corners of the mud walls were observed as the displacement angle increased over 1/50 rad. Except for the shear failure that suddenly appeared on the top of the left column at 1/10 rad, there was no significant damage observed at mortise-tenon joints, and there was no clearly shear failure in the middle part of the hanging mud walls. The damage state of both specimens is shown in Figure 6.

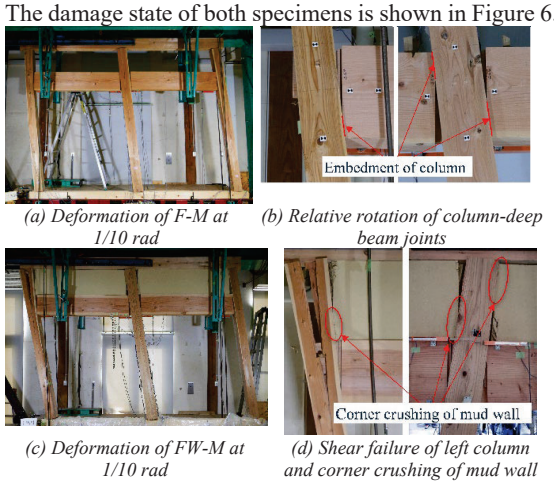

(a) Deformation of F-M at 1/10 rad

(b) Relative rotation of column-deep beam joints

(c) Deformation of FW-M at 1/10 rad

(d) Shear failure of left column and corner crushing of mud wall

Figure 6: *Damage state of F-M and FW-M at 1/10 rad.*

For specimens FW-S and FW-L which contain hanging mud walls of different heights, the most significant differences between the two frames at the displacement angle of 1/10 rad are the failure mode of hanging mud walls (Figure 7). For hanging mud walls with a height aspect ratio of 0.19 in FW-S, no significant shear failure was observed. Except for crushes at the left and right corners, vertical cracking occurred at the upper and lower surfaces of the mud wall at about 1/4 length from the edge. For hanging mud walls with a height aspect ratio of 0.56 in FW-L in contrast, diagonal cracks occurred from the interior area of both mud walls and expanded towards the edge. And because of the more obvious lifting effect of mud walls, the crushing failures of upper and lower surfaces at the wall corners were observed. In addition, bending deformation of the side columns was also more significant than that in FW-S, due to the greater shear

https://doi.org/10.52202/069179-0527

force transmitted by hanging mud walls and closer action position to the mid-span of columns.

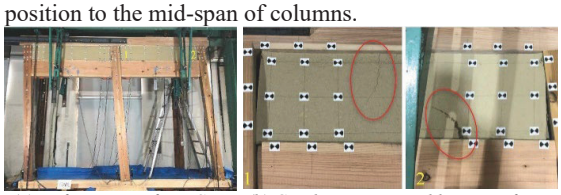

(a) Deformation of FW-S at 1/10 rad *(b) Cracks at upper and lower surface of mud walls*

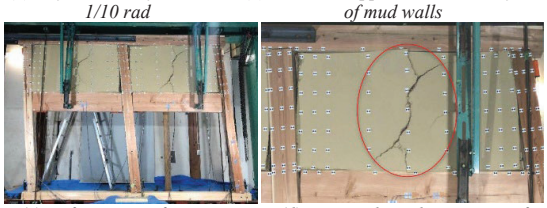

(c) Deformation of FW-L at 1/10 rad *(d) Diagonal cracks at center of mud walls*

Figure 7: *Damage state of FW-S and FW-L at 1/10 rad.*

3.1.2 Restoring characteristics

The restoring force characteristics of four frame specimens, and the main damage with corresponding displacement angles are shown in Figure 8. By comparing the skeleton curves of specimens F-M and FW-M, the contribution of hanging mud walls to the lateral resistance of the frame can be extracted (Figure 9(a)). When the hanging mud walls with a centreline height of 750 mm are included, the initial rigidity is increased by 1.57 times compared to the bare timber frame. After the peak value of lateral force reaches 15.73 kN at 0.06 rad, the load-carrying capacity of the FW-M slowly decreases with the occurrence of corner crushing of mud walls. In contrast, the lateral force added on F-M maintains an upward trend and reaches 13.11 kN at 0.1 rad, which is very close to that of FW-M.

From the perspective of the influence of wall height on the lateral resistance of the frame (Figure 9(b)), the initial rigidity of FW-L is 2.5 times higher than that of FW-S, and the peak load is also 1.34 higher. However, after the shear cracks occurred at 1/15 rad, the bearing capacity of FW-L decreased rapidly. As for FW-S, as the height aspect ratio of hanging mud walls is small and there is no shear failure occurs, the integral frame can maintain a stage lateral resistance even under large deformation. The result indicates that although the shear area of hanging mud walls remained the same, the stiffness as well as bearing capacity of the frame are positively correlated with the height of hanging mud walls.

The structural indices of frame specimens calculated according to the design method of JHWTC [4] as shown in Figure 9, including initial rigidity K, yield load P_y, maximum load P_{max}, ultimate load P_u, ductility factor μ, and short-term allowable lateral force P_a are listed in Table 3. P_a of the frame with different heights of hanging mud walls is derived by Eq. (1).

$$P_a = \alpha \cdot \min \begin{cases} P_y \\ 0.2\sqrt{(2\mu - 1)}P_u \\ 2/3 \cdot P_{max} \\ P_{120} \end{cases} \quad (1)$$

in which P_{120} is the lateral force at displacement angle of 1/120 rad, $\alpha = 1.0$.

Table 3: *Structural indices of frame specimens.*

Frame	K (kN/rad)	P_y (kN)	P_u (kN)	P_{max} (kN)	μ	P_a (kN)
F-M	362.46	7.60	11.79	13.11	3.08	3.83
FW-M	568.05	9.26	14.38	15.73	3.94	5.56
FW-S	408.31	11.11	17.08	19.53	2.32	3.73
FW-L	1026.95	18.47	22.94	26.14	4.57	8.99

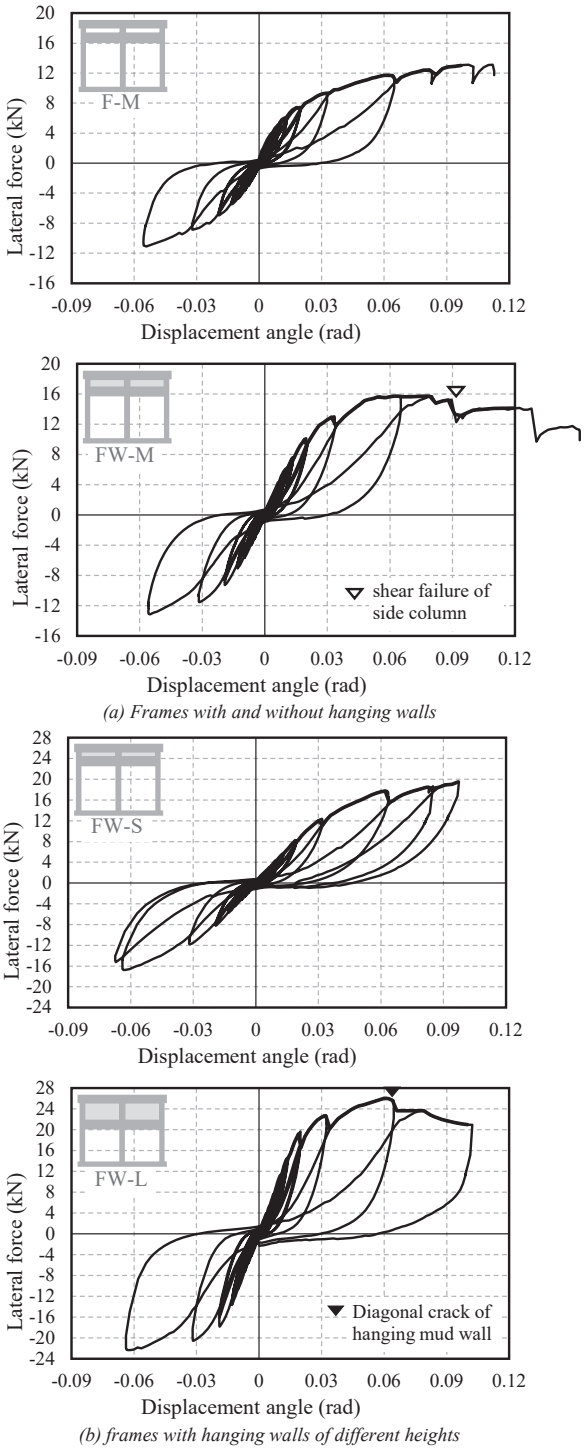

(a) Frames with and without hanging walls

(b) frames with hanging walls of different heights

Figure 8: *Restoring characteristics of frame specimens.*

https://doi.org/10.52202/069179-0527

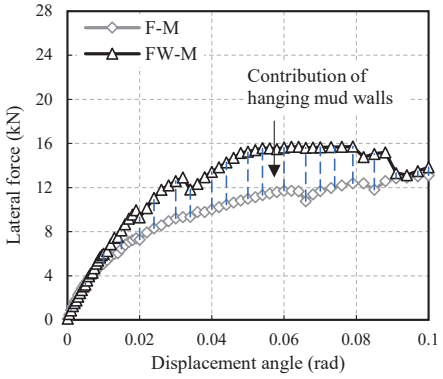

(a) Frames with and without hanging walls

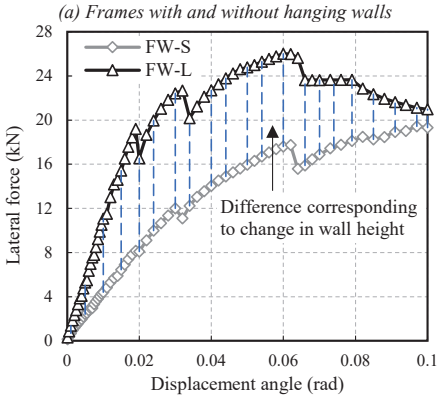

(b) frames with hanging walls of different heights

Figure 9: *Skeleton curves of frame specimens.*

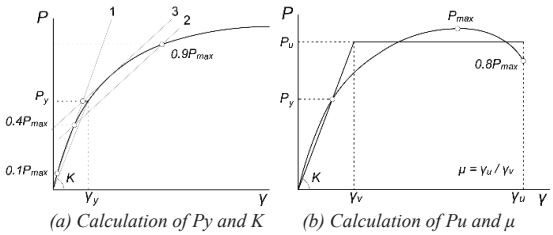

(a) Calculation of Py and K *(b) Calculation of Pu and μ*

Figure 10: *Calculation procedure of structural indices [4].*

3.2 PERFORMANCE OF MAIN COMPONENTS IN THE FRAME

Based on the lateral force-deformation relationship obtained from elemental tests, the contributions of main load-bearing components, including the mortise-tenon joints (Q_{Fj}), deep beams (Q_{Fb}), and hanging mud walls (Q_{Fw}), are extracted from the entire frame. The burden ratio of them is shown in Figure 11. It is observed that the resistance proportion of mortise-tenon joints exceeds 60% when the centerline height of the hanging mud wall is less than 750 mm. For hanging mud walls, the resistance proportion of which is positively correlated to the wall height, the peak occurs at about 0.02 rad and then begins to decline. The resistance proportion of deep beams in the bare timber frame accounts for about 10-15%, while in frames with hanging mud walls, its resistance is manifested when the displacement angle is above 0.02 rad.

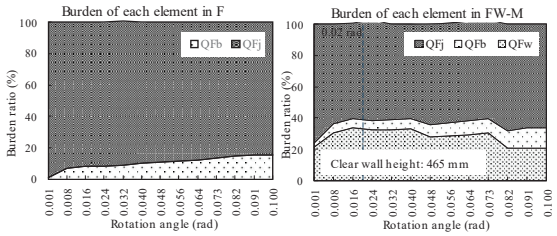

(a) Frames with and without hanging walls

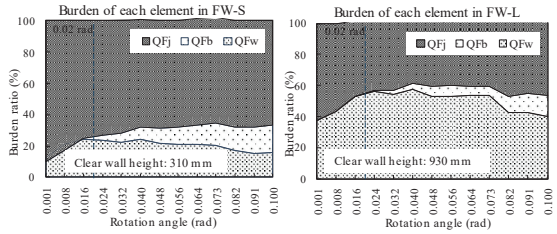

(b) frames with hanging walls of different heights

Figure 11: *Burden ratio of each element in frame specimens.*

3.2.1 Interaction between mortise-tenon joints and deep beams

By comparing the results of the frame and elemental tests, the interaction between beam-column joints and deep beams is identified.

Firstly, from the experimental phenomenon, the displacement angle corresponding to shear damage of the column-deep beam joints in the frame tests is greater (0.1 rad) than that in joint elemental tests (0.06 rad). This is mainly caused by the compression effect generated by the rotation of the deep beam clamped between two columns, which delays the tenon removal. From the moment-displacement angle curve extracted from the frame, it can be seen that the initial rigidity of the column-deep beam joint in the frame is lower than that in elemental tests (Figure 12(a)). And due to the failure delay of mortise-tenon joints, the overall resistance of the frame can maintain an increasing trend at 0.1 rad. Conversely, due to the pressure generated by the rotation of the beam end joint being partially balanced by the tensile force generated by the dowel, the axial force transmitted along the diagonal direction of the deep beam decreases (Figure 12(b)).

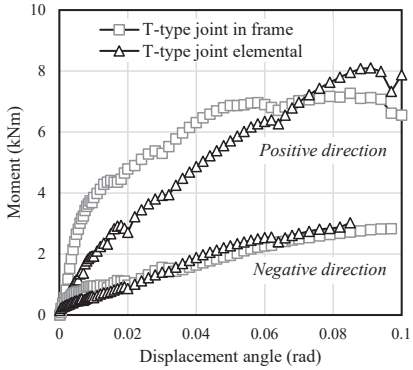

(a) Moment of T-type joint with and without influence of deep beams

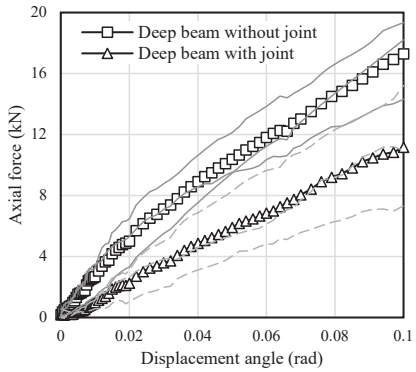

(b) Axial force on deep beams with and without influence of joints

Figure 12: *Interaction between deep beams and joints.*

3.2.2 Performance of hanging mud walls

Based on the elemental tests of squat mud walls, a positive correlation between the resistance of squat mud walls and the height aspect ratio is confirmed when the height aspect ratio is lower than 0.5 (Figure 13). Furthermore, the resistances generated by shear and corner compression are extracted respectively.

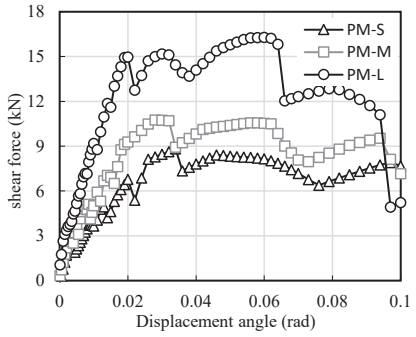

Figure 13: *Shear resistance of squat mud walls.*

3.2.3 Bending performance of columns

Although there was no bending failure occurred on the columns of both FW-S and FW-L specimens, the bending moments measured from the center and the leeward side columns of FW-L significantly increased as the concentrated load transmitted by hanging mud walls increased. Based on the comparative bending tests of columns with and without mortise at the loading point, the reduction coefficient β of bending moment (Eq. (2)), affected by the stress concentration of mortise is calculated. The experimental result shows that when the width lost ratio on the tensile side is lower than 0.4, the mean value of β is obtained as 1.0. Compared with the much lower coefficient (β=0.45~0.6) in the regulations in AIJ standard [5], it can be inferred that the continuous part out of the mortise plays an important role in relieving stress concentration.

$$M_{b-M} = \alpha \cdot \beta \cdot M_{b-0} \quad (2)$$

in which M_{b-0} is the bending moment of columns without mortise, M_{b-M} is the bending moment of columns with mortise, α is the nominal section modulus, calculated by the ratio between the weakest net section of mortise and the entire section.

4 CONCLUSIONS

The presented work focused on the lateral performance of a frame with deep beams and hanging mud walls in traditional Japanese residential houses. With the change of wall height, the initial rigidity, yield load, and ductility of the entire frame, as well as the resistance contribution of moment-resisting joints, deep beams, and hanging mud walls were evaluated.

The experimental results indicate that for the timber frame with deep beams and hanging mud walls, the lateral rigidity and lateral load-bearing capacity are positively correlated with the increase of the height of hanging mud walls. Regardless of whether the shear failure occurs on the hanging mud wall, its burden ratio of lateral force contribution reaches the peak at 0.02 rad. The collaborative working mechanism of mortise-tenon joints and deep beams ensures the good ductility of the entire frame. For the timber frame with the wall centerline height below 750 mm, the contribution of mortise-tenon joints to the lateral resistance accounts for over 60%.

ACKNOWLEDGEMENT

This study is one of the items of the project for the promotion and maintenance for building standards by MLIT.

REFERENCES

[1] Komatsu K., Kitamori A., Jung K., and Mori T.: Prediction of Non-linear Load-deformation Curves of Various Types of Mud Shear Walls Subjected to Lateral Shear Force. In 11th World conference on timber-engineering, 2708-2715, 2010.

[2] Official gazette co-operation of Japan. No. 1100 Notification of Ministry of Land, Transport and Tourism Infrastructure. In *Technical standard of building structure*, 111-121, 2020. (in Japanese)

[3] Japan building disaster prevention association (JBDPA). Guidance for seismic assessment and reinforcement method of timber residences. *Maeda print.co.jp,* 18-50, 2012. (in Japanese)

[4] Japan housing and wood technology center (HWTC). Design of allowable stress of wooden frame construction housing. *Japan housing and wood technology center, Tokyo,* 571-572, 2008. (in Japanese)

[5] Architectural institute of Japan, AIJ standard for Structural Design of Timber structures. *Maruzen publishing Inc*, *Tokyo*, 188-193, 2006. (in Japanese)

https://doi.org/10.52202/069179-0527